Available online at www.sciencedirect.com
ScienceDirect
Cellular Signalling 20 (2008) 1104–1116
CELLULAR SIGNALLING
www.elsevier.com/locate/cellsig

cAMP-induced Epac-Rap activation inhibits epithelial cell migration by modulating focal adhesion and leading edge dynamics

Karen S. Lyle [a,1,2], Judith H. Raaijmakers [a,2], Wytse Bruinsma [a], Johannes L. Bos [a,*], Johan de Rooij [b,*]

[a] Department of Physiological Chemistry, Centre for Biomedical Genetics and Cancer Genomics Centre, Universiteitsweg 100, 3584 CG Utrecht, the Netherlands
[b] Department of Cell Biology, the Netherlands Cancer Institute, Plesmanlaan 121, 1066 CX, Amsterdam, the Netherlands

Received 22 November 2007; received in revised form 18 January 2008; accepted 18 January 2008
Available online 31 January 2008

Abstract

Epithelial cell migration is a complex process crucial for embryonic development, wound healing and tumor metastasis. It depends on alterations in cell–cell adhesion and integrin–extracellular matrix interactions and on actomyosin-driven, polarized leading edge protrusion. The small GTPase Rap is a known regulator of integrins and cadherins that has also been implicated in the regulation of actin and myosin, but a direct role in cell migration has not been investigated. Here, we report that activation of endogenous Rap by cAMP results in an inhibition of HGF- and TGFβ-induced epithelial cell migration in several model systems, irrespective of the presence of E-cadherin adhesion. We show that Rap activation slows the dynamics of focal adhesions and inhibits polarized membrane protrusion. Importantly, forced integrin activation by antibodies does not mimic these effects of Rap on cell motility, even though it does mimic Rap effects in short-term cell adhesion assays. From these results, we conclude that Rap inhibits epithelial cell migration, by modulating focal adhesion dynamics and leading edge activity. This extends beyond the effect of integrin affinity modulation and argues for an additional function of Rap in controlling the migration machinery of epithelial cells.

Keywords: Rap; Epac; cAMP; Migration; Integrin; Cytoskeleton

1. Introduction

Epithelial cell migration is a complex process induced by specific growth factors that takes place during certain stages of embryonic development, organogenesis and wound healing. In response to oncogenic signals, epithelial cell migration also mediates tumor invasion and metastasis [1]. Epithelial cell migration requires the disruption of cell–cell adhesion [1], the modification of the integrin–extracellular matrix (ECM) interactions [2] and engagement of the actomyosin-based migration machinery that induces polarized membrane protrusion [3]. Beneath this leading edge protrusion of a migrating cell, integrin-mediated focal contacts are initiated and subsequently reinforced by tension generated in the actomyosin cytoskeleton [4]. As a consequence, they grow larger and alter their composition to become focal adhesions (FAs) [5]. Contraction of the actomyosin cytoskeleton attached to leading edge FAs pulls the cell body forward and is used to disassemble rear-end FAs [6,7]. The efficiency of migration in two-dimensional culture also depends on the balance between ECM concentration and the extent of integrin-activation [8].

Several growth factors implicated in tumor metastasis can induce the processes described above in cultured cells, resulting in the scattering of initially clustered epithelial cells. The most well-known inducers of epithelial cell scattering are transforming growth factor-β (TGFβ) and hepatocyte growth factor (HGF) [9]. TGFβ induces scattering in many different cell lines,

* Corresponding authors. J. de Rooij is to be contacted at Hubrecht Institute, Uppsalalaan 8, 3584 CT, The Netherlands. Tel.: +31 30 2121960; fax: +31 30 2126464.
E-mail addresses: j.l.bos@umcutrecht.nl (J.L. Bos), j.derooij@niob.knaw.nl (J. de Rooij).
[1] Current address: Wittmann Laboratory, Department of Cell and Tissue Biology, University of California-San Francisco, 513 Parnassus Avenue, HSW-618, San Francisco, CA, United States.
[2] These authors contributed equally to this paper.

0898-6568/$ - see front matter © 2008 Elsevier Inc. All rights reserved.
doi:10.1016/j.cellsig.2008.01.018

invariantly accompanied by silencing of the E-cadherin gene through Smad signaling [10]. The most prominent induction of scattering by HGF occurs in MDCK cells [11] and does not involve down regulation of E-cadherin protein levels or adhesive capacity, but correlates with increased integrin-mediated adhesion and depends on actomyosin based tension [12]. Given the lethal consequences of tumor metastasis, we aim to understand the cellular machinery that governs epithelial cell migration.

cAMP is a pivotal second messenger that regulates a wide range of cellular processes. Signaling through cAMP and protein kinase A (PKA) has been implicated in cytoskeletal regulation and cell migration [13]. The effects of PKA on cell migration can be both stimulatory and inhibitory, depending on the cell type and matrix used [13–16]. cAMP also activates the guanine nucleotide exchange factor (GEF) Epac that can subsequently activate the small GTPase Rap [17]. Rap is an important regulator of both integrin- and cadherin-mediated adhesion (reviewed in [18–20]). Although it is not yet completely understood how Rap regulates these two processes, several proteins that interact with its GTP-bound form have been identified that may serve as effector proteins [18]. In the case of integrin-mediated adhesion, Rap regulates both integrin affinity and integrin avidity, or clustering, depending on the type of integrin and the cell type [21–24]. Two effectors of Rap1, Riam and RapL, have been shown to be important in the regulation of integrin affinity [25,26], although they induce integrin activation via distinct mechanisms [27,28]. In the regulation of (V)E-cadherin-mediated adhesion, Rap effectors likely recruit junctional proteins to sites of developing cell–cell contacts to stabilize the connection between the actin cytoskeleton and the junctional complex [20,29,30]. Because of its established function as a regulator of integrin-mediated cell adhesion, a role for Rap in cell migration has been suggested. Direct evidence comes from studies in leukocytes, where chemokine-induced integrin activation by Rap1 leads to an increase in adhesion to the endothelium and subsequent endothelial transmigration [31,32]. Clearly, in addition to PKA, also Epac/Rap signaling may be involved in regulation of cell migration via cAMP.

Previously, we reported that Rap is involved in cell surface expression of E-cadherin and the stabilization of cell–cell junctions and that cAMP-induced activation of Rap through Epac1 inhibits HGF-induced cell scattering. These observations suggested that scattering is inhibited by stabilization of adherens junctions [33]. However, a deficiency in C3G, another RapGEF, results in increased migration velocity [34], indicating that Rap might also have a restraining effect on cell migration itself. Moreover, Zhang et al. recently described that TGFβ-induced transformation of cells is inhibited by cAMP, independently of PKA [35]. As TGFβ, in contrast to HGF, down regulates the E-cadherin expression levels, cAMP-Epac-Rap signaling may regulate cell migration directly rather than through a stabilizing effect on cell–cell junctions.

Here, we show that activation of Rap through Epac1 inhibits epithelial cell migration in a number of different model systems in response to both HGF and TGFβ, irrespective of the presence of cell–cell junctions. Interestingly, forced integrin activation, by the integrin-activating antibody TS2/16, does not inhibit migration, even though it induces adhesion to the ECM to the same extent as Rap activation does. Apparently, the effects of Rap on cadherin-mediated adhesion and integrin activation are not sufficient to inhibit epithelial cell migration, indicating that inhibition of the basal cell migration machinery is the critical step downstream of Rap that mediates its effects on scattering. To further understand the mechanism of Rap-induced inhibition of cell migration, we studied the migration machinery in more detail and observed that Rap activation impairs the dynamics of focal adhesions and blocks protrusive activity at the leading edge in migrating cells. These effects are also not mimicked by integrin activating antibodies. Together, these data show that Rap regulates focal adhesion and leading edge dynamics, independently of integrin activation, to restrain epithelial cell migration.

2. Results

2.1. cAMP-induced Rap activation inhibits HGF-stimulated epithelial cell migration

To investigate the effect of Rap activation on epithelial cell migration we used MDCK cells, which do not express endogenous Epac, and MDCK cells stably expressing GFP-tagged human Epac1 (MDCK-GFP-Epac cells). Cells were plated in a 48-well plate coated with collagen (10 μg/mL), simultaneously filmed by phase-contrast microscopy for 2 h, stimulated with HGF, and filmed for an additional 18 h. Parental MDCK cells exhibited a typical response to HGF; the cells initially spread, disrupted cell–cell contacts and migrated away from their neighbors (Movie S1 and Fig. 1A). MDCK-GFP-Epac cells showed a similar response to HGF treatment compared to parental MDCK cells, but scattering was inhibited in HGF-stimulated MDCK-GFP-Epac cells treated with the cell-permeable cAMP analogue 8-bromo-cAMP (Movie S1 and Fig. 1A) or the cAMP-elevating drug forskolin (Movie S2 and Fig. S1). 8-Bromo-cAMP did not inhibit scattering in parental MDCK cells, suggesting that activation of Epac mediated this response. To confirm that PKA is not needed for the inhibition of scattering by cAMP, we used the Epac-specific cAMP analog 8-CPT-2OMe-cAMP [36] and the PKA-specific cAMP analog N6-Bnz-cAMP [37]. 8-CPT-2OMe-cAMP inhibited scattering in MDCK-GFP-Epac, but not in parental MDCK cells (Movie S1 and Fig. 1A). In contrast, activation of PKA with N6-Bnz-cAMP did not inhibit scattering in MDCK-GFP-Epac cells (Movie S2 and Fig. S1).

To quantify these observations, the migration velocity of parental and MDCK-GFP-Epac cells was determined by tracking cell nuclei using custom-written, automated cell-tracking software. For each condition 3 independent time-lapse image series were analyzed, resulting in the tracking of at least 300 individual cells per condition. MDCK and MDCK-GFP-Epac cells increased their migration velocity from 0.5 to 1.2 μm/min, within 16 h of HGF stimulation (Fig. 1B, solid and dashed black lines). MDCK cells treated with 8-bromo-cAMP showed the same response to HGF (Fig. 1B, solid grey line). In contrast, MDCK-GFP-Epac cells exposed to HGF and 8-bromo-cAMP or 8-CPT-2OMe-cAMP showed no significant increase in cell velocity (Fig. 1B, grey dashed line and Fig. 1C, black dashed line,

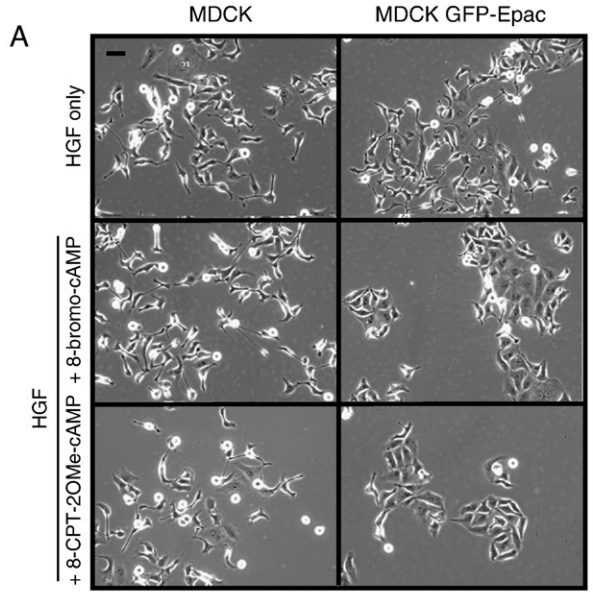
A
MDCK
MDCK GFP-Epac
HGF only
HGF
+ 8-bromo-cAMP
+ 8-CPT-2OMe-cAMP

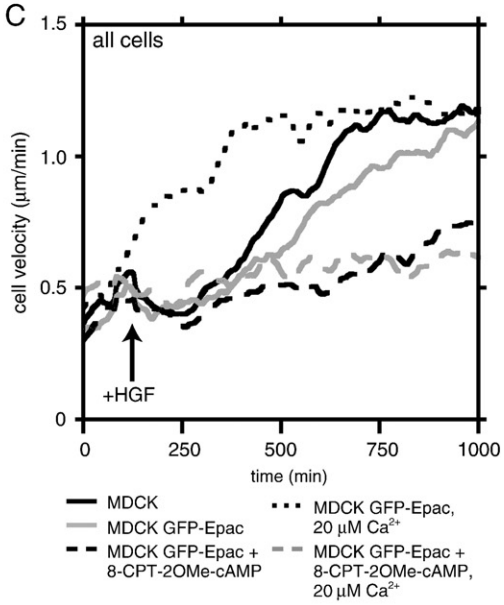
C
all cells
cell velocity (μm/min)
time (min)
+HGF
MDCK
MDCK GFP-Epac
MDCK GFP-Epac + 8-CPT-2OMe-cAMP
MDCK GFP-Epac, 20 μM Ca2+
MDCK GFP-Epac + 8-CPT-2OMe-cAMP, 20 μM Ca2+

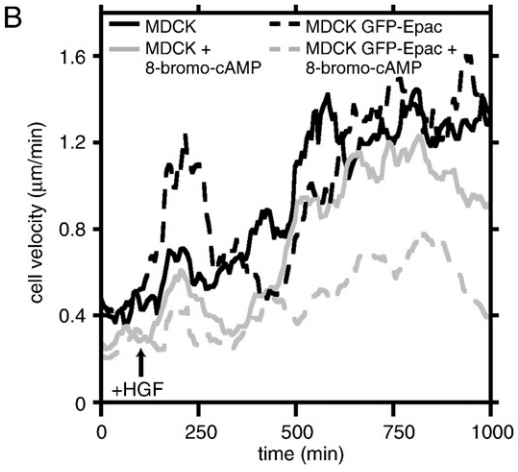
B
MDCK
MDCK + 8-bromo-cAMP
MDCK GFP-Epac
MDCK GFP-Epac + 8-bromo-cAMP
cell velocity (μm/min)
time (min)
+HGF

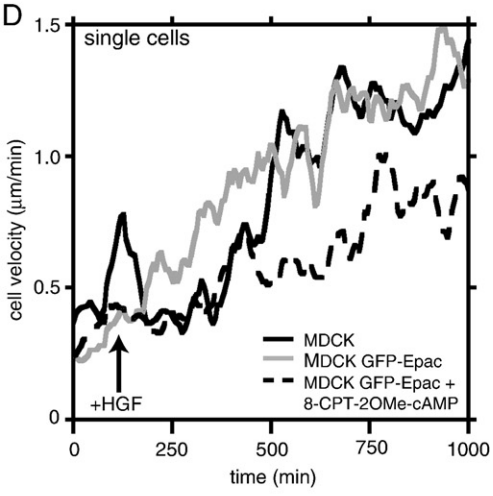
D
single cells
cell velocity (μm/min)
time (min)
+HGF
MDCK
MDCK GFP-Epac
MDCK GFP-Epac + 8-CPT-2OMe-cAMP

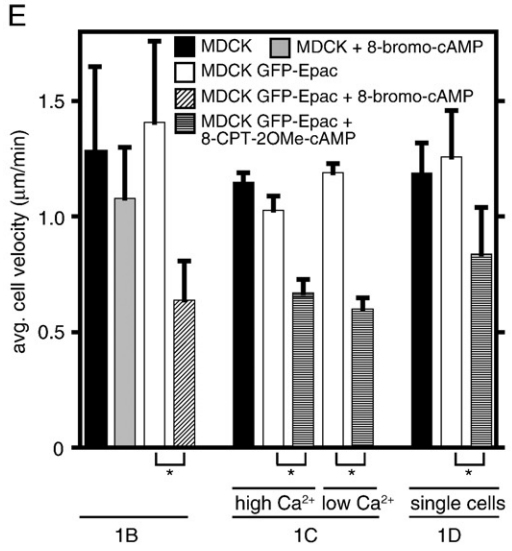
E
MDCK
MDCK + 8-bromo-cAMP
MDCK GFP-Epac
MDCK GFP-Epac + 8-bromo-cAMP
MDCK GFP-Epac + 8-CPT-2OMe-cAMP
avg. cell velocity (μm/min)
high Ca2+
low Ca2+
single cells
1B
1C
1D

respectively). To evaluate the statistical significance of the inhibition of migration by cAMP, the velocity values for each time point after the plateau of maximal velocity was reached (t=750–1000 min post-HGF) were averaged (Fig. 1E) and subjected to a Students t-test. Thus we conclude that cAMP-induced activation of Epac (and not PKA) and subsequent activation of endogenous Rap in MDCK cells strongly inhibits HGF-induced scattering.

2.2. Rap activation inhibits HGF-induced cell migration in the absence of cell–cell junctions

As Rap has been previously shown to modulate both cell–cell and cell-ECM adhesion receptors [21–23,33,38,39], we aimed to investigate whether the cAMP-induced inhibition of cell migration is simply caused by the stabilization of cell–cell adhesion through Rap. To this end, we analyzed the velocity of MDCK-GFP-Epac cells in the absence of cell–cell junctions using two approaches. First, we examined the HGF-induced motility in low Ca^{2+} (20 μM Ca^{2+})-containing medium that does not support homotypic E-cadherin adhesion. Second, we used our tracking software to distinguish clearly single cells from cells in contact with neighboring cells in high Ca^{2+} conditions to specifically analyze the HGF-induced motility of single cells.

Fig. 1C (dotted black line and Movie S3) shows that HGF-stimulated MDCK-GFP-Epac cells in low Ca^{2+}-containing medium achieved a similar maximum velocity of 1.2 μm/min. Notably, these cells showed an earlier increase in cell velocity compared to MDCK-GFP-Epac cells cultured in high Ca^{2+} (Fig. 1C, solid grey line), indicating that cell–cell junctions do need to be disrupted before the velocity increase is observed. In the presence of 8-CPT-2OMe-cAMP, MDCK-GFP-Epac cells in low Ca^{2+} showed no increase in velocity, similar to 8-CPT-2OMe-cAMP-treated cells in the presence of high Ca^{2+} (Fig. 1C, dashed grey and dashed black lines, respectively and Movie S3). To corroborate this conclusion, the velocity increase of clearly non-contacted cells present in high Ca^{2+} conditions (usually less than 10% of all cells) was inhibited as well (Fig. 1D, dashed black line). Comparison of maximum velocities and statistical analysis was performed as above and is depicted in Fig. 1E. These data demonstrate that Rap activation strongly inhibits epithelial cell migration even in the absence of functional adherens junctions.

2.3. Rap inhibits epithelial cell migration induced by several different growth factors

To investigate if the inhibitory effect of Rap activation on cell migration is restricted to HGF-induced motility, we used A549 cells that scatter in response to HGF or TGFβ, another notorious metastasis-promoting growth-factor [40] that disrupts cell–cell junctions by silencing the E-cadherin gene [10]. In analogy to MDCK cells, we constructed a cell line stably expressing Epac1 (A549-Epac, Fig. 2A) to specifically activate endogenous Rap by 8-CPT-2OMe-cAMP. As shown in Fig. 2B, both HGF and TGFβ induce scattering in A549 and A549-Epac cells. In A549-Epac cells, scattering is abolished by 8-CPT-2OMe-cAMP, whereas in parental A549 cells scattering is normal.

We used time-lapse phase-contrast microscopy to further characterize the scattering process and the effect of Rap activation on it in these cells (Movie S4) and measured cell migration to quantify this. HGF and TGFβ both induce cell migration (Fig. 2C, solid black and grey lines, respectively), which is completely abolished by 8-CPT-2OMe-cAMP (Fig. 2C, dotted black and grey lines, respectively). Quantification and statistical evaluation is shown in Fig. 2E. Thus, Rap activation efficiently blocks scattering induced by two distinct signaling pathways, one of which results in a loss of E-cadherin expression (even in the presence of active Rap, see Fig. 3F).

2.4. cAMP induction of endogenous Epac-Rap signaling inhibits epithelial cell migration

To investigate whether endogenous Epac-Rap signaling also blocks cell migration, we used renal cell carcinoma RCC10 cells. These cells are Von Hippel–Lindau-defective and express little to no E-cadherin [41]. RCC10 cells respond to HGF stimulation by activating ERK1/2 and express the β1 integrin required for migration on a collagen matrix, as well as Epac1 (Figs. 2A and 3C). These cells showed a 1.5 fold increase in velocity upon HGF stimulation (Fig. 2D, solid black line and Movie S5). The motogenic response of these cells was more rapid compared to MDCK cells, and cells achieved their maximal velocity after 1 h of HGF stimulation. This probably reflects the absence of cell–cell junctions in these cells. Importantly, treating cells with 8-CPT-2OMe-cAMP to specifically activate Epac/Rap, completely inhibited the HGF-induced increase in cell motility (Fig. 2D, dotted black line and Movie S5 and quantification in 2E). Together, these data show that cAMP-mediated activation of endogenous Rap via both exogenously- and endogenously-expressed Epac1 leads to the inhibition of epithelial cell scattering induced in different cell lines and by different growth factors. As this inhibition is independent of the level of E-cadherin expression and the presence of cell–cell junctions, this suggests that Rap has an inhibitory effect on the induction of cell migration itself.

Fig. 1. cAMP-induced Rap activation inhibits HGF-induced cell migration in the absence or presence of cell–cell adhesion. (A) Representative images from phase contrast timelapse image series showing the inhibitory effect of 8-bromo-cAMP and 8-CPT-2OMe-cAMP on HGF-induced cell motility in MDCK-GFP-Epac, but not parental MDCK cell lines. Scale bar is 100 μm. (B) Velocity time-course, by automated tracking of approximately 300 cells from three independent time-lapse image series, to quantify HGF-induced migration and cAMP-induced inhibition in these cells. (C) Velocity time-course by tracking of approximately 600 cells from 3 independent time-lapse image series to quantify the inhibitory effect of 8-CPT-2OMe-cAMP on HGF-induced MDCK and MDCK-GFP-Epac cell velocity in the presence (1.8 mM Ca^{2+}) and absence (20 μM Ca^{2+}) of cell–cell junctions. (D) Velocity time-course by tracking of approximately 60 cells from 3 independent time-lapse image series, showing the effect of 8-CPT-2OMe-cAMP on the migration of non-contacted MDCK-GFP-Epac cells in high Ca^{2+}. (E) Average cell velocity (averaging values from all time-points at the plateau phase of maximum velocity (750–1000 min)) (±SD) from each of the velocity time-courses in B, C, and D. An asterisk (*) indicates $p<0.0001$.

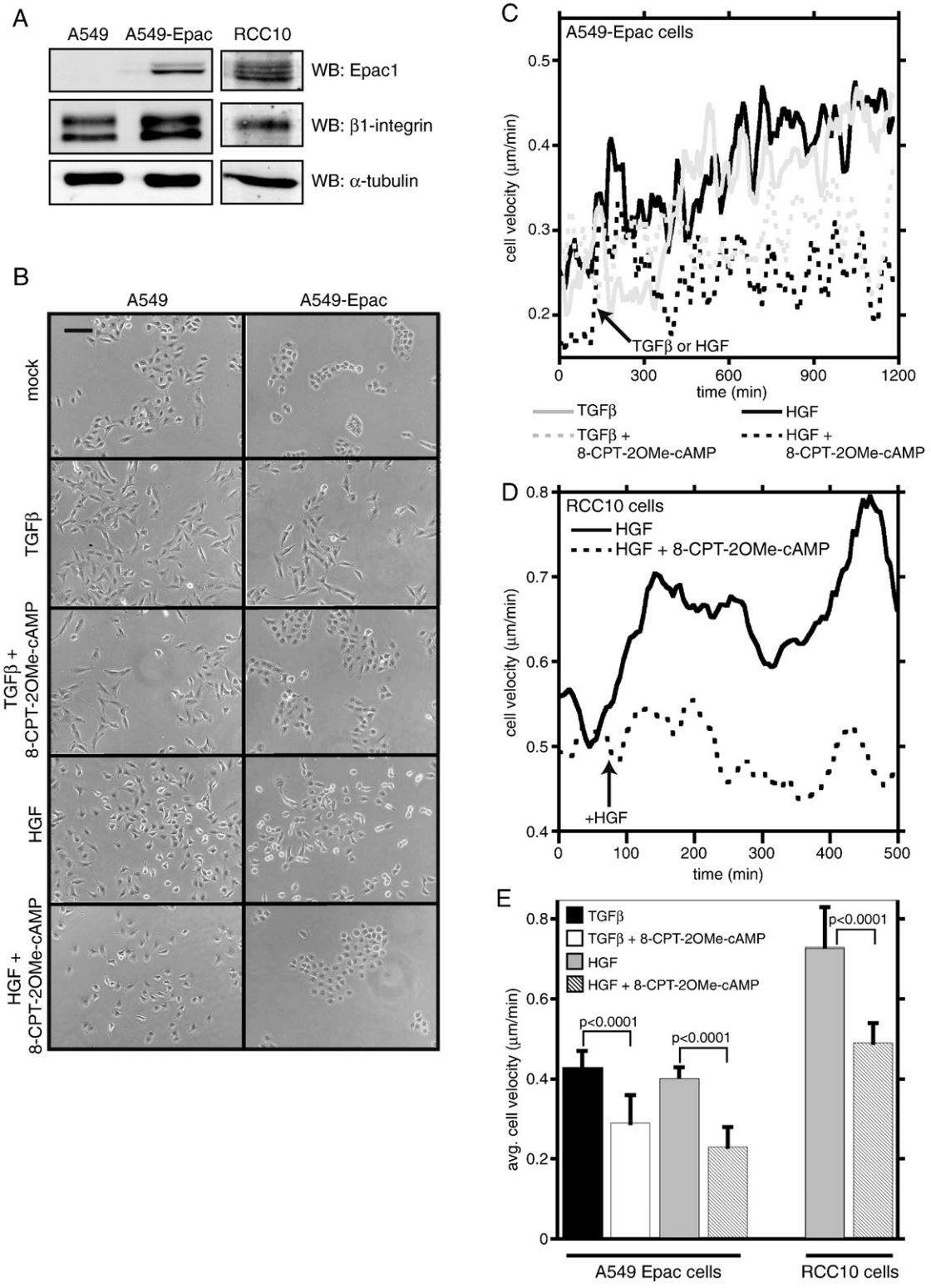

Fig. 2. Rap activation inhibits several types of growth factor-induced epithelial cell migration. (A) Western blot showing Epac1 and β1-integrin expression in A549-Epac and RCC10 cells. (B) 8-CPT-2OMe-cAMP inhibits TGFβ- and HGF-induced scattering of A549-Epac cells. Representative phase contrast images of A549-Epac cells showing the effect of 8-CPT-2OMe-cAMP on TGFβ- and HGF-induced cell scattering. Scale bar is 100 μm. Cells were stimulated with TGFβ or HGF for 24 h, in the presence or absence of 8-CPT-2OMe-cAMP. (C) Velocity time-course showing the effect of 8-CPT-2OMe-cAMP on TGFβ- and HGF-induced A549-Epac cell migration. (D) Velocity time-course showing the inhibitory effect of 8-CPT-2OMe-cAMP on HGF-induced RCC10 cell migration. (E) Average cell velocity (±SD) at the plateau phase (1100–1200 min) of A549 cells and RCC10 cells (400–500 min) from each of the velocity time-courses in C and D, respectively.

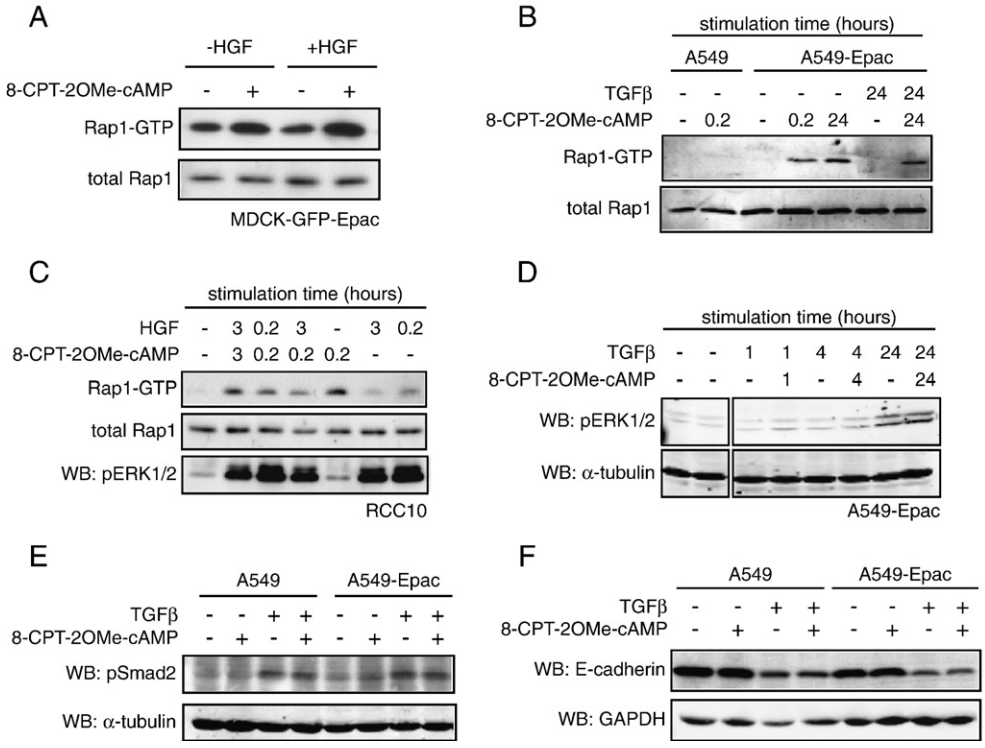

Fig. 3. Rap activation does not interfere with growth factor signaling. (A) Rap is activated by 8-CPT-2OMe-cAMP in MDCK-GFP-Epac cells in the presence and absence of HGF. Cells were stimulated for 16 h with HGF and/or 8-CPT-2OMe-cAMP. Blots shown are representative of at least 3 independent experiments. (B) Rap activation in parental and Epac-expressing A549 cells. Cells were treated for the indicated time periods with TGFβ and 8-CPT-2OMe-cAMP prior to performing a Rap-GTP pulldown assay. Blots shown are representative of at least 4 independent experiments. (C) Rap activation does not interfere with HGF-induced ERK activation and 8-CPT-2OMe-cAMP-induced Rap activity is not significantly affected by short- or long-term HGF stimulation in RCC10 cells. Cells were treated for the indicated time periods with HGF and/or 8-CPT-2OMe-cAMP prior to performing a Rap-GTP pulldown assay and probing of whole cell lysates for Erk activation. Blots shown are representative of 3 independent experiments. (D) Rap activation does not affect TGFβ-induced ERK activation in A549-Epac cells. Cells were incubated for 24 h with the indicated stimuli. Whole cell lysates were probed with the appropriate antibodies as indicated to show activation and equal loading. Blots shown are representative of at least 3 independent experiments. (E) Epac expression and Rap activation do not affect TGFβ-induced phosphorylation of Smad2. Cells were incubated for 24 h with the indicated stimuli. Whole cell lysates were probed with the appropriate antibodies as indicated to show activation and equal loading. Blots shown are representative of 3 independent experiments. (F) Rap activation does not restore TGFβ-induced downregulation of E-cadherin in A549-Epac cells. Cells were incubated for 24 h with the indicated stimuli. Whole cell lysates were probed with the appropriate antibodies as indicated to show activation and equal loading. Blots shown are representative of at least 3 independent experiments.

2.5. 8-CPT-2OMe-cAMP activates Rap, but does not interfere in growth factor signaling

One of the mechanisms via which Rap may interfere in growth factor-induced cell migration, is through direct inhibition of growth factor signaling. Rap pulldowns were used to confirm that 8-CPT-2OMe-cAMP activates Epac to induce Rap-GTP in Epac-expressing (endogenous or exogenous) cell lines. This activation of Rap was present for the complete duration of our time lapse experiments and was not affected by HGF or TGFβ stimulation (Fig. 3A–C). Next, we examined if Epac1 expression or Rap activation with 8-CPT-2OMe-cAMP could suppress HGF- and TGFβ-mediated ERK activation [40]. In agreement with our previous experiments in MDCK cells [33], activation of Rap in RCC10 cells does not interfere with HGF-induced ERK1/2 phosphorylation at any of the time-points investigated (Fig. 3C). Rap activation also did not modulate the TGFβ-induced phosphorylation of ERK1/2 in A549-Epac cells (Fig. 3D). Furthermore, neither exogenous Epac1 expression nor 8-CPT-2OMe-cAMP stimulation suppressed Smad2 phosphorylation after TGFβ addition (Fig. 3E), as was reported in 293T cells [42]. Finally, Rap activation did not affect the down regulation of E-cadherin protein levels that is observed in the presence of TGFβ (Fig. 3F). These data show that Rap activation does not interfere in the major growth factor receptor signaling events important for scattering, but rather acts to prevent the induction of migration at a more downstream level. For instance, Rap may directly inhibit the migration machinery.

2.6. Forced integrin activation does not mimic the inhibitory effects of Rap on cell migration

Besides the disruption of cell–cell adhesion [1], cells also require modification of the integrin-mediated adhesion to the ECM [2] and engagement of the actomyosin-based migration machinery that induces polarized membrane protrusion [3] for efficient cell migration. To investigate whether the induction of integrin affinity downstream of Rap [21,28], could explain the inhibition of cell migration, we examined the effect of integrin-activating antibodies on HGF-induced cell motility. These antibodies force the integrins

into their high-affinity conformation and thus mimic inside-out integrin activation as induced by Rap. Because these antibodies recognize human, but not dog integrins, we used RCC10 and A549 cells and not MDCK cells. For RCC10 cells plated on collagen, which mainly binds to β1 integrins to mediate cell migration, we used the β1 integrin-activating antibody TS2/16 [43]. For A549 cells plated on fibronectin (Fn), which can bind to β1 and β3 integrins to facilitate cell migration, we used a combination of TS2/16 and the β3 integrin-activating antibody LIBS6 [8,44]. In short-term adhesion assays performed with RCC10 cells on collagen, TS2/16 and 8-CPT-2OMe-cAMP induce adhesion to a similar extent (Fig. 4C), indicating that indeed β1 integrins are the main collagen receptors in these cells. In A459 cells on Fn, TS2/16 induces adhesion to a higher extent than 8-CPT-2OMe-cAMP, whereas LIBS6 results in a very small induction of adhesion (Fig. 4F), indicating that β1 integrins are the main receptors for Fn in these cells. However, in migration experiments TS2/16 did not inhibit HGF-induced cell motility in RCC10 cells (Fig. 4A, solid grey line), and TS2/16+LIBS6 failed to inhibit HGF-induced migration in A459 cells (Fig. 4D, solid grey line). Quantification of

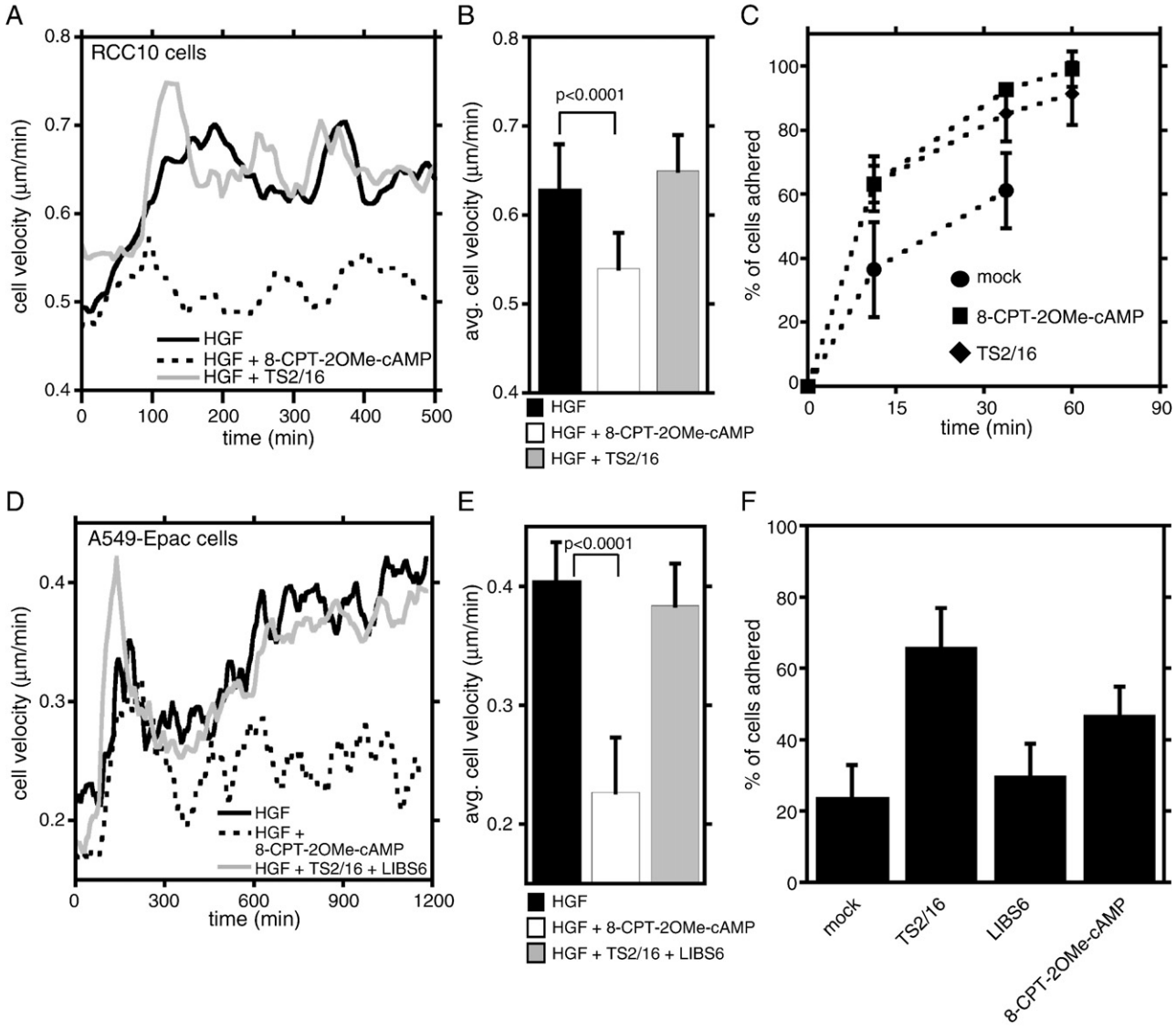

Fig. 4. Forced integrin-activation by antibodies does not mimic the effect of Rap activation on cell migration. (A) Velocity increase of RCC10 cells by HGF is inhibited by 8-CPT-2OMe-cAMP, but not TS2/16. In a live-cell phase-contrast time-lapse, HGF and 100 μM 8-CPT-2OMe-cAMP or 3 μg/ml TS2/16 were added at $t=60$ min. Velocity of approximately 300 automatically tracked cells from 3 independent time-lapse image series was measured. (B) Average cell velocity (±SD) of RCC10 cells at the plateau-phase (400–500 min) from the velocity time-course in A. (C) Adhesion time course showing comparable 8-CPT-2OMe-cAMP- and TS2/16-induced adhesion kinetics in RCC10 cells on 3 μg/ml collagen. Cells were plated in the absence or presence of 100 μM 8-CPT-2OMe-cAMP or 3 μg/ml TS2/16 and left to adhere for the indicated time points. Data are means±SD; $n=4$. (D) Velocity increase of A549-Epac cells by HGF is not inhibited by TS2/16 and LIBS6. HGF and 100 μM 8CPT-2OMe-cAMP or antibodies (3 μg/ml TS2/16 and 3.7 μg/ml LIBS6) were added during imaging at $t=120$ min and velocity was determined by automated cell-tracking of approximately 300 cells from 3 independent time-lapse image series. (E) Average cell velocity (±SD) at the plateau-phase (1100–1200 min) of A549 cells from the velocity time-course in C. (F) TS2/16 and 8-CPT-2OMe-cAMP, but not LIBS6, induce adhesion of A549-Epac cells to fibronectin. A549-Epac cells were plated on 1 μg/ml fibronectin in the absence or presence of 100 μM 8-CPT-2OMe-cAMP or 3 μg/ml TS2/16 or 3.7 μg/ml LIBS6, allowed to adhere for 30 min, washed and quantified. Data are means±SD; $n=4$.

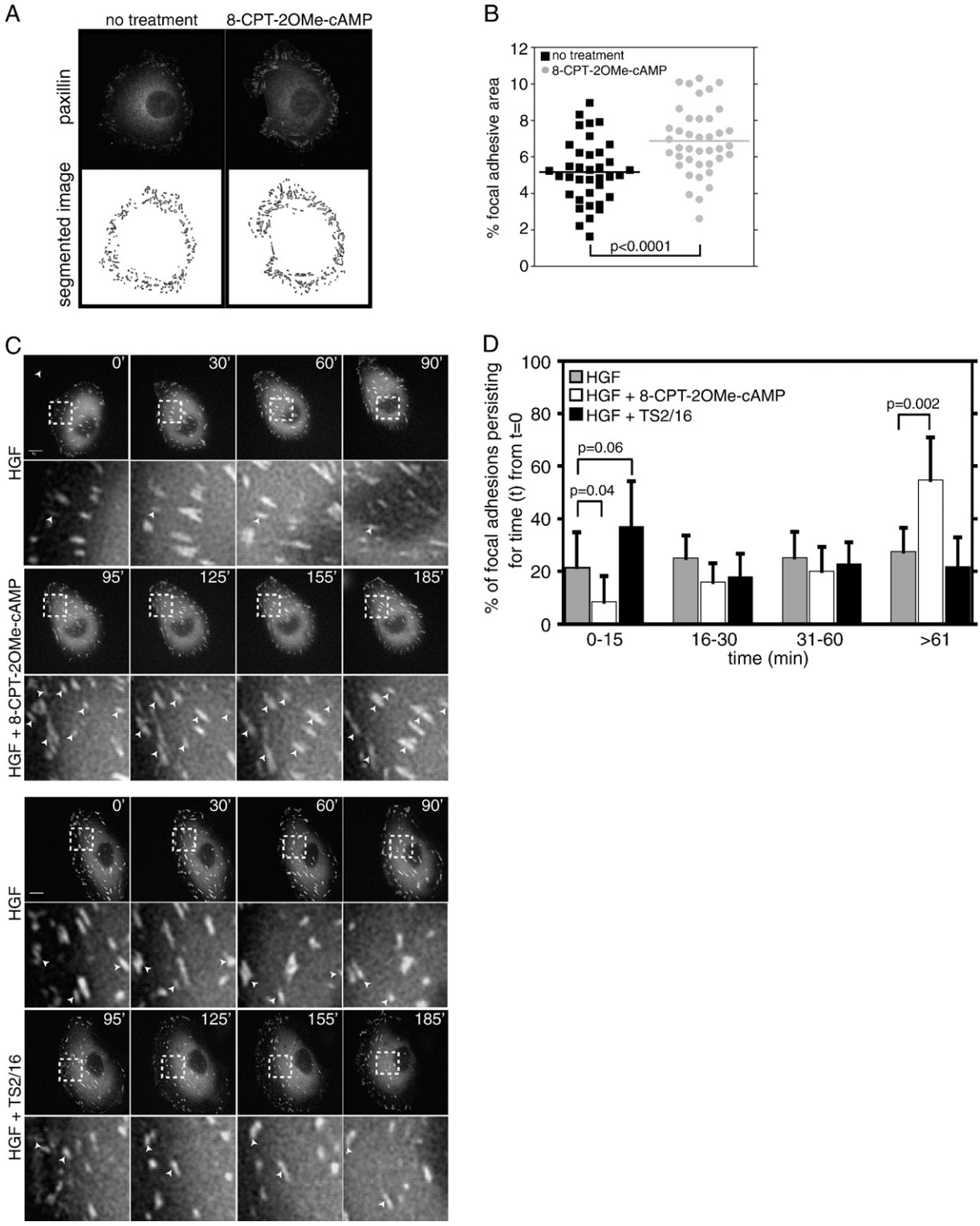

Fig. 5. Rap activation enhances focal adhesion area and stability. (A) Representative images showing the effect of 8-CPT-2OMe-cAMP on FAs in MDCK-Epac cells. Cells were plated on collagen in the presence or absence of 8-CPT-2OMe-cAMP, fixed and stained for paxillin. Lower panels show images segmented in ImageJ. (B) Images were processed and the total focal adhesion and cell area for at least 35 cells from 2 independent experiments were quantified in ImageJ as described in the Materials and methods section. (C) Representative images from timelapse series showing the effect of 8-CPT-2OMe-cAMP and TS2/16 on the stability of GFP-paxillin-labeled FAs in HGF-treated RCC10 cells. A 7.6 μm × 7.6 μm area of the cell is highlighted (white dashed box), and white arrowheads show FAs that persist for more than 60 min within this area. Scale bar is 5 μm. (D) Focal adhesion persistence analysis was performed in ImageJ as described in the Materials and methods section for eight cells (~200 FAs tracked per condition) and the data are expressed as the mean ± SD.

plateau-velocity and statistical evaluation is shown in Fig. 4B (RCC10 cells, 400–500 min) and 4E (A549 cells, 1100–1200 min). This shows that simply inducing integrin activation does not inhibit HGF-induced motility and indicates that a different effect downstream of Rap is involved.

2.7. Rap activation inhibits focal adhesion turnover and front-rear polarity in contrast to forced β1-integrin activation

Because just simple integrin activation and ECM adhesion does not seem to be enough to inhibit migration, we focused on focal adhesions (FAs), to investigate if Rap might affect integrin signaling downstream of the integrin-ECM connection. FAs regulate cell motility by connecting the cytoskeleton to the ECM [45]. To determine if Rap activation modulates these structures in epithelial cells, we examined the effect of 8-CPT-2OMe-cAMP on FA morphology in MDCK-Epac cells (MDCK cells stably expressing un-tagged Epac1 [33]) plated on collagen and stained for paxillin, a major component of FAs. Three hours after plating, MDCK-Epac cells (in the absence or presence of 8-CPT-2OMe-cAMP) were adhered and spread onto the collagen-coated glass coverslip. In the presence of 8-CPT-2OMe-cAMP, FAs were larger and more elongated and paxillin staining was more intense (Fig. 5A). The same effect on focal adhesion area was observed in A549-Epac and RCC10 cells (data not shown). Measuring the area of paxillin intensity that clearly surmounted background fluorescence, revealed a 1.3-fold increase in the relative focal adhesion area in 8-CPT-2OMe-cAMP-treated compared to untreated cells (Fig. 5B, $p<0.0001$). These data show that Rap activation enhances FAs in MDCK-Epac cells.

Next, we examined the dynamic behavior of FAs in migrating RCC10 cells. For these studies we used RCC10 cells because they express endogenous Epac, exhibit a rapid response to HGF and do not form tightly clustered cell colonies. RCC10 cells were transfected with GFP-paxillin, plated and imaged using widefield fluorescence microscopy. Cells transfected with GFP-paxillin appeared indistinguishable from untransfected cells in phase-contrast images demonstrating that exogenous GFP-paxillin expression does not significantly alter the morphology of RCC10 cells (data not shown). In the presence of HGF, we observed small FAs forming at the leading edge of protrusions, and larger FAs in the body and trailing edge of the cell (Movie S6 and Fig. 5C (panels from 0 to 90 min)). In Fig. 5C, a dashed grey box outlines a magnified region at the leading edge of the cell, and white arrowheads identify the FAs that persist for longer than 60 min. Upon stimulation with 8-CPT-2OMe-cAMP, cells rapidly altered their focal adhesion dynamics with fewer FAs forming and disappearing within the 90 min time period (Fig. 5C, panels from 95 min onwards and Movie S6), resulting in a loss of small leading edge adhesions and an increase in large central FAs. As a consequence, cells appeared to rapidly lose their distinct front/rear polarity and migration was inhibited, when stimulated with 8-CPT-2OMe-cAMP, but not with TS2/16.

The lifetime of individual FAs is highly variable in migrating cells. To quantify focal adhesion lifetime in a comprehensive manner, we randomly selected FAs in the first frame of the image sequence and determined how long these persisted. Cells treated with HGF showed a nearly equal percentage of FAs that persisted for a short time (less than 15 min), intermediate times (16–60 min) and a very long time (>61 min) (Fig. 5D). When Rap was activated in these cells, the percentage of FAs lasting for more than 61 min was increased 2-fold (Fig. 5D, grey and white bars, $p=0.002$), whereas we observed a concomitant 2-fold decrease in the percentage of FAs lasting 15 min or shorter ($p=0.04$). TS2/16 treatment did not mimic the effect of 8-CPT-2OMe-cAMP, as it did not result in any increase in the percentage of long-lasting FAs, but rather in a 1.5-fold increase of small, short-lived FAs (Fig. 5C and D, grey and black bars, $p=0.06$). Furthermore, the presence of TS2/16 enhanced the polarized phenotype of these cells (as judged by the asymmetric distribution of small and large FAs).

In conclusion, Rap activation reduces FA dynamics and results in the loss of front rear polarity. This response is very different from the response to treatment with an integrin-activating antibody, which shows increased FA dynamics and no loss of cell-polarity.

2.8. Rap activation reduces lamellipodial activity

In RCC10 GFP-paxillin timelapses, we noted a decrease in the number of leading edge protrusions after Rap activation (Fig. 6A, arrowheads). To clearly determine whether Rap activation indeed affects HGF-induced protrusion and retraction, we examined the membrane dynamics of RCC10 cells in the presence and absence of 8-CPT-2OMe-cAMP. RCC10 cells were transiently transfected with the membrane marker GFP-CAAX [46], plated on collagen-coated glass-bottom dishes overnight and imaged using widefield fluorescence microscopy. In the presence of HGF, RCC10 cells formed approximately equivalent and polarized areas of net protrusion and retraction (Fig. 6B, solid black areas and Movie S7). The total protrusion and retraction area was markedly reduced when Rap was activated with 8-CPT-2OMe-cAMP in HGF-treated cells (Fig. 6B), but remained in cells treated with TS2/16. Furthermore, protrusion and retraction were not polarized in 8-CPT-2OMe-cAMP-treated cells as no persistence in any direction was observed. These differences were not due to toxic or otherwise disturbing effects of the expression of GFP-CAAX as expression was similar in HGF-only and HGF+8-CPT-2OMe-cAMP or HGF+TS2/16-treated cells used for this analysis (as determined by fluorescence intensity). Furthermore, HGF-only treated cells that expressed GFP-CAAX migrated indistinguishable from untransfected RCC10 cells (data not shown).

To quantify the protrusive activity, we divided the area of leading-edge extension in consecutive frames by the total cell area during the 60 min of the experiment (Fig. 6C). The average membrane activity of HGF-treated cells was 1.4-fold higher than basal activity (Fig. 6C, black and grey lines, respectively, and 6D). The membrane activity was reduced 1.4-fold when Rap was activated with 8-CPT-2OMe-cAMP (Fig. 6C, black dashed line and 6D). Addition of TS2/16 antibody only resulted in a small difference in protrusive activity (Fig. 6B and C, grey dashed line, and 6D) and polarization was fully maintained. Clearly, forced integrin activation by TS2/16 did not mimic the inhibitory effect of Rap activation. These data demonstrate that Rap activation blocks the

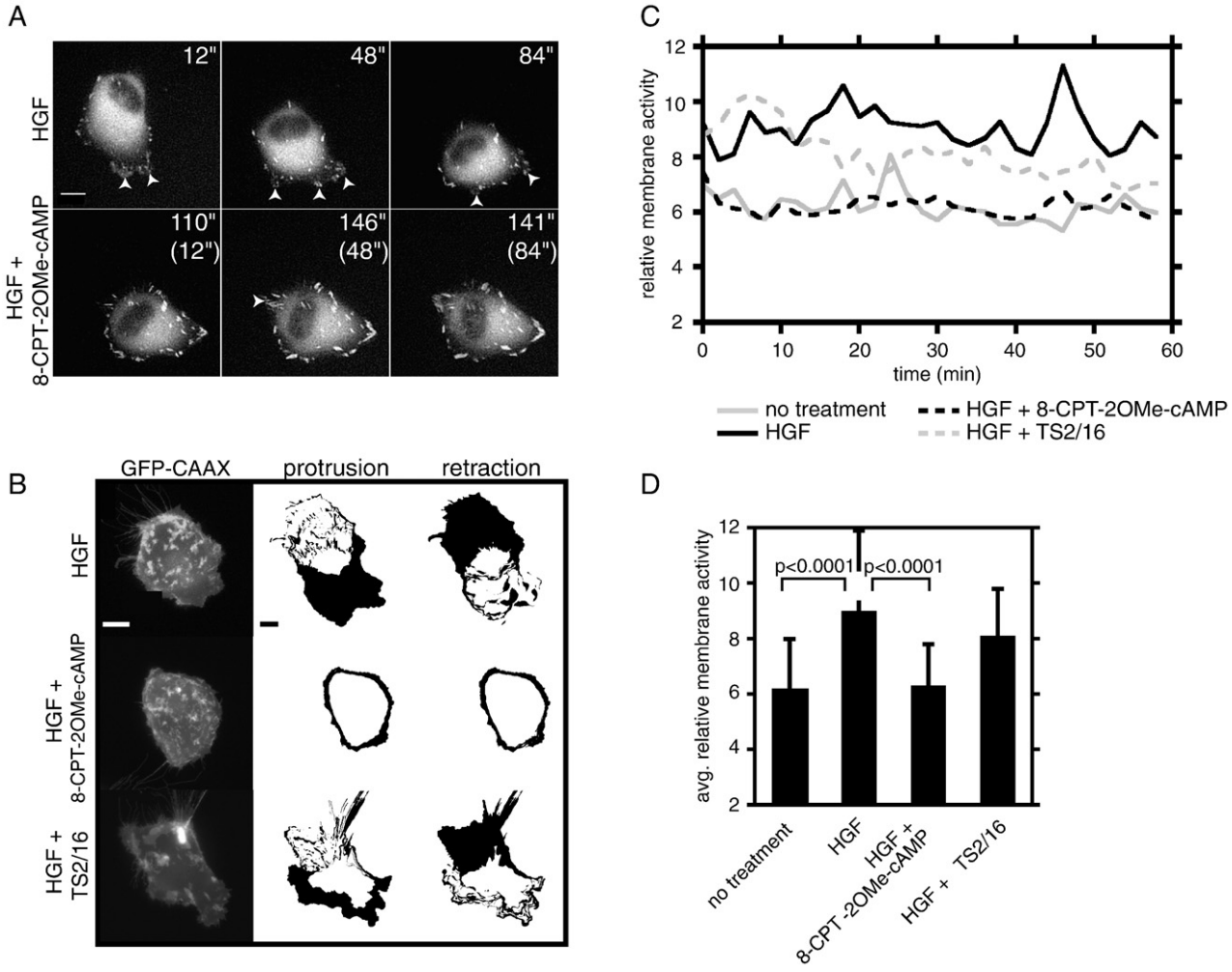

Fig. 6. Rap activation inhibits HGF-induced membrane protrusions. (A) 8-CPT-2OMe-cAMP decreases the number of protrusions in RCC10 cells treated with HGF. The arrowheads indicate newly formed protrusions in GFP-paxillin expressing RCC10 cells in each timelapse frame. (B) Rap activation reduces the HGF-induced increase in membrane protrusion and retraction area. Representative images of RCC10 cells transiently expressing GFP-CAAX and their corresponding total protrusion and retraction area (black areas) over 60 min after treatment with HGF alone, HGF+8-CPT-2OMe-cAMP, and HGF+TS2/16. The difference in membrane area between sequential timelapse images was determined in ImageJ as described in the Materials and methods section. Scale bar is 5 μm. (C) Timecourse showing the difference in membrane area relative to the total area of the cell, due to protrusion and retraction, in sequential frames of 60 min timelapses. The data are the averages from 9, 27, 18, and 19 cells for mock-, HGF-, HGF+8-CPT-2OMe-cAMP-, and HGF+TS2/16-treated cells, respectively. (D) Average membrane activity (±SD) of RCC10 cells during the time-course in C.

HGF-induced increase in polarized membrane protrusion and retraction.

3. Discussion

For cells to migrate efficiently, both cell–cell junctions and cell-ECM interactions need to be regulated and tension within the actomyosin cytoskeleton needs to be induced [1–3]. Polarized membrane protrusion and efficient turnover of focal adhesions are also required for efficient cell migration [6]. As the small GTPase Rap is a known regulator of cell junctions and integrin-mediated adhesion [18] and has been suggested to be involved in cell migration [34], we investigated how Rap interferes in epithelial cell migration. Surprisingly, neither the stabilization of cell–cell junctions nor the activation of integrins could account for this effect on migration. Major receptor signaling pathways like ERK and Smad (unlike previously reported [42]), are also not affected, indicating that signaling through Epac/Rap does not interfere in HGF or TGFβ signaling, but rather acts downstream to block the induction of cell migration by these transforming growth factors.

During migration on the ECM, integrin-based FAs provide linkage between the cytoskeleton and the ECM to transmit forces, sense the environment and initiate intracellular signaling cascades [45]. Regulated, efficient formation and turnover of FAs is required for optimal cell migration. Small adhesions at the leading edge turn over rapidly to facilitate protrusion or mature into larger FAs that provide the tension for the disassembly of adhesions at the rear of the cell [6,47].

We examined the effect of Rap activation on FAs using paxillin as a marker [48] and found a rapid alteration of focal adhesion dynamics. After Rap was activated, fewer FAs formed at the leading edge and focal adhesion disassembly was inhibited,

resulting in an overall increase in FA persistence and an apparent loss of the polarized morphology that is characteristic of migrating cells. One explanation for the observed effects on focal adhesion complexes is an increase in integrin-mediated cell adhesion. However, the β1-integrin-activating antibody TS2/16 did not affect FA dynamics in the same way as Rap activation, although both induced a similar level of adhesion. This suggests that increased integrin-affinity per se is not causing the inhibition of cell migration. In accordance with these observations, Huttenlocher et al. showed that forcing integrins into a high affinity state using antibodies does not influence FA morphology and does not strongly inhibit cell migration, but shifts the optimal migration conditions to a lower concentration of ECM substrate. In contrast, mutant integrins that have lost proper regulation of their linkage to the cytoskeleton and exhibit forced cytoskeletal linkage, show strongly enhanced FAs and a severely impaired capacity to migrate [8]. We observe similar effects when Rap is activated in epithelial cells that are treated with growth factors. Our results, therefore, suggest that Rap has an effect on the integrin-cytoskeletal linkage and that this effect is more important for the inhibition of cell migration than the effect of Rap on integrin affinity. Whether this is achieved by the same molecules that mediate the affinity modulation (Riam and Talin [28]), remains to be shown. Thus far we could not detect endogenous Riam or Riam-GFP in FAs in the cells that we used for our experiments.

In addition to stabilizing FAs, Rap inhibits the formation of polarized membrane protrusions during migration. This process is driven by actin polymerization (the motor), but also depends on a regulation of the integrin-cytoskeletal linkage (the clutch) as has been illustrated by two recent papers [49,50]. Several reports have indicated that Rap may influence actin polymerization, the driving force behind lamellipodial protrusion. For instance, Rap has strong stabilizing effects on cortical actin in endothelial cells [51,52] and the Rap interacting protein RIAM was shown to increase the amount of filamentous actin, presumably through its interaction with profilin [25]. Furthermore, Rap interacts with several RacGEFs, known regulators of actin polymerization, to increase cell-spreading [53], although it has also been reported that Rap can function as an antagonist of Rac signaling [54].

Because we also observe an effect on FA dynamics, the effect of endogenous Rap activity on lamellipodial protrusion could be explained by a stabilization of the connection between the integrins and the cytoskeleton. In other words, the clutch is engaged too long, leading to a loss of productive protrusion. Further studies are required to determine whether Rap regulates the connection between the actin cytoskeleton and integrins and to identify the molecular mechanism that mediates the Rap-induced inhibition of cell migration.

Finally, contractile tension generated within the actomyosin cytoskeleton is also required for efficient migration. Increased actomyosin contraction results in increased FA size [45] and dynamic regulation of myosin is critical to efficient protrusion [55]. An alternative explanation for the effects on FA size and dynamics and for the effects on protrusion could be the recent finding that Rap1 regulates myosin in Dictyostelium [56]. However, we could not detect any effects of Rap activation on myosin light chain phosphorylation downstream of HGF or TGFβ, arguing against this possibility. Also, the Rap1 effector that mediates the myosin induction by Rap1 is not conserved between Dictyostelium and mammals.

4. Conclusion

We conclude that activation of endogenous Rap leads to an inhibition of growth factor-induced epithelial cell migration by targeting the basal migration machinery. This effect is independent of E-cadherin stabilization and cannot be explained solely by affinity modulation of β1-integrins. Rap inhibits epithelial cell migration through the stabilization of focal adhesions and the inhibition of membrane protrusion, possibly by stabilizing the connection between the actin cytoskeleton and integrins.

5. Materials and methods

5.1. Cell lines and culture

Stable MDCK-GFP-Epac cells were created by transfection of MDCK with pEGFP-C1-Epac1 followed by selection with G418. Polyclonal MDCK cells stably expressing moderate levels of GFP-Epac were isolated by fluorescence activated cell sorting (FACS) from this cell line. MDCK-Epac1 cells were described previously [33]. Stable Epac1-expressing A549 cells were created by infecting A549 cells with Epac1 ecotrophic virus. The Epac1 gene was linked via an IRES sequence to a zeocin resistance gene. Forty-eight hours after infection, cells were placed under selection with zeocin (0.2 mg/ml) to select for Epac1 expressing cells. Monoclonal A549-Epac1 cell lines expressing moderate levels of Epac1 were single-cell sorted from these polyclonal cell lines by FACS. MDCK, MDCK-GFP-Epac and MDCK-Epac cells were cultured in DMEM supplemented with 10% fetal calf serum (FCS), glutamine, and antibiotics. A549 and RCC10 cell lines were cultured in RPMI supplemented with glutamine, antibiotics, and 10% or 8% FCS, respectively. RCC10 cells were transiently transfected using Fugene transfection reagent (Roche) according to the manufacturer's protocol. Cells were plated in complete medium 24 h after transfection, and analysis of expressed proteins occurred 24 h thereafter.

5.2. Plasmids

The GFP-CAAX construct expresses an N-terminal GFP-tagged tetra-amino acid motif (CAAX) that localizes to the plasma membrane [46]. The GFP-paxillin construct expresses an N-terminal EGFP-tagged fusion to human paxillin and was generously provided by Dr. Marc Ginsberg (University of California-San Diego). GFP-Epac1 contains amino acids 2-881 of Epac1 fused at its N-terminus to EGFP in the pEGFP-C1 vector.

5.3. ECM proteins

For analysis of MDCK cell motility, non-tissue culture treated 48-well plates were coated with collagen type I from calf skin (Sigma) for 2 h at 37 °C, washed 3 times with phosphate buffered saline (PBS), and blocked with 1% heat-denatured bovine serum albumin (BSA) in PBS for 1 h at 37 °C. For analysis of A549 cell motility, 48 well plates were coated with 1 μg/mL fibronectin for 2 h at 37 °C and washed 3 times in PBS. In all other cases, glass-bottomed dishes and coverslips were coated with collagen type I from rat tendon (Upstate) for 16 h at 4 °C and washed 3 times in PBS.

5.4. Rap activation assays and immunoblotting

Rap activation was assayed as described previously [57]. Endogenous Rap was detected following Western blotting with polyclonal anti-Rap antibody (Santa Cruz). Polyclonal phospho-ERK (Thr202/Tyr204) antibody and phospho-Vasp (Ser157) antibody were obtained from Cell Signaling. Polyclonal phospho-Smad2

(Ser465/467), monoclonal anti-E-cadherin (HECD-1) and anti-GAPDH antibodies were from Chemicon International. Anti-β1 integrin and anti-β-catenin antibodies were from BD Transduction Laboratories and anti-tubulin antibody was from Calbiochem. Monoclonal anti-Epac1 5D3 antibody was described previously [33].

5.5. Live cell microscopy

For phase-contrast imaging, MDCK, MDCK-GFP-Epac, and RCC10 cells were plated in medium containing 0.5% FCS and 10 mM Hepes, pH 7.4, 24 h before image acquisition in non-tissue culture–treated polystyrene well plates coated with 10 μg/mL collagen (or the indicated concentrations). Prior to imaging, 100 μM 8-CPT-2OMe-cAMP, 10 μM forskolin, 300 μM N6-Bnz-cAMP or 3 μg/mL TS2/16 were added to the appropriate wells, wells were completely filled with medium and the plate was sealed using silicon grease and a glass plate. Images were acquired every 6 min using a 10×0.5 NA Plan objective lens and a 0.5 NA ELWD condenser with a Zeiss Axiocam camera on a Zeiss Axiovert 200 M microscope in climate-controlled incubator. A robotic stage (Zeiss MCU 28) was used to collect images at different stage positions. All electronic microscope functions were controlled using Axiovision software (Zeiss). The cells were imaged for 2 h in absence of HGF, and then 5 ng/ml HGF was added to cells on the microscope stage to prevent loss of the cells of interest and imaging was continued for 16 h. At least three timelapse series were acquired for each condition in each separate experiment.

A549 and A549-Epac cells were plated on a fibronectin-coated (1 μg/mL) 48-well plate 24 h before imaging, which was performed as above. At the indicated timpoint 10 ng/mL TGFβ, 25 ng/ml HGF and 100 μM 007 or 3 μg/ml integrin-activating antibody TS2/16 and/or LIBS6 were added to the appropriate wells. GFP-tagged proteins were imaged in an 8-well Lab-tek chambered coverglass (Nalge Nunc International, Rochester, NY) coated with 10 μg/mL collagen on a Zeiss Axiovert 200 M microscope using a Lambda DG-4 Ultra High Speed Wavelength Switcher from Sutter Instruments as a light source. Fluorescent images were acquired every 2 or 3 min using either a 40X/1.3 oil or a 63X/1.25 oil Neofluar objective lens.

5.6. Fixation and immunolocalization

Cells were fixed in freshly-prepared 4% paraformaldehyde for 10 min, permeabilized in 0.2% Triton X-100 for 5 min, and blocked in PBS containing 0.2% BSA and 5% horse serum for 1 h at room temperature. Cells were incubated with monoclonal paxillin antibody (BD Biosciences) for 1 h in PBS containing 0.2% BSA, followed by incubation with the appropriate secondary antibody for 45 min at room temperature. Images were acquired using a Zeiss Axioskop 2 microscope fitted with a Zeiss Axiocam CCD camera and 100X Plan APO objective lens.

5.7. Image analysis and processing

To determine cell trajectories in phase-contrast timelapse image series, the centroids of the nuclei were followed. To automate this and allow for unbiased analysis of many cells in multiple timelapses, a program was written in Matlab (Mathworks) that segments images based on pixel intensity and determines the presence of nuclei based on phase-density, size and shape. Nuclei are then linked in consecutive frames using a neural network algorithm and cells tracked for less than 5 consecutive frames are automatically discarded (manuscript in preparation, JdR and Danuser G.). Detection fidelity in our experiments was over 80%, which was confirmed by eye for each individual timelapse. To distinguish single cells from clustered cells in this program, areas occupied by cells were determined by edge-detection and overlayed with the detected nuclei to determine if one (single cell) or more (clustered cells) nuclei were present in a detected cell-area. Similar results were obtained when a smaller number of randomly selected cells from a number of timelapses were analyzed using the track objects function in MetaMorph (Universal Imaging Corp.).

Focal adhesion and total cell areas from images of fixed and stained cells were measured in ImageJ. First, the fluorescence intensities of images from 2 independent experiments were normalized, and then a bandpass filter was applied to remove background staining that was consistently observed around the nucleus. FAs were segmented using the analyze particles function in ImageJ, and the total segmented area was normalized to the total cell area. The effectiveness of our segmentation procedure was inspected visually.

FAs were manually tracked in ImageJ. Approximately 27 FAs were randomly selected in similarly localized regions of the cell and marked in the first frame ($t=0$) of each timelapse series using the Cell Counter ImageJ plugin. The selected FAs were tracked until they were no longer visible and the frame at which the focal adhesion disappeared was recorded.

To quantify protrusion dynamics, we determined the changes in membrane area between sequential timelapse images of RCC10 cells expressing GFP-CAAX. Using Metamorph software, an exclusive threshold was applied to each normalized image series to define the outer cell membrane. We created a journal in Metamorph that defined and measured the thresholded areas and produced a stack of binary images. The subtract function in the ImageJ Image Calculator was applied to sequential binary timelapse images to determine areas of protrusion and retraction, and differences in membrane area were normalized to the total cell area. Images showing the net protrusion and retraction were made by applying the sum slices option in the z-project function of ImageJ to sequentially subtracted images.

5.8. Adhesion assays

Cells were trypsinized, washed once in RPMI containing 10% FCS, and allowed to recover surface proteins for 1.5 h in suspension in RPMI containing 0.5% FCS, glutamine, antibiotics, and 10 mM Hepes, pH 7.4, at 37 °C with constant, gentle rolling. 8-CPT-2OMe-cAMP (200 μM) and TS2/16 antibody (2 μg/mL, unless indicated otherwise) were diluted in 100 μL of RPMI and added to the wells of a 48-well polystyrene cell culture dish coated with 3 μg/ml collagen (for RCC10 cells) or 1 μg/ml fibronection (A549-Epac cells). After rolling, 50,000 cells in 100 μL were plated per well, making the final concentrations of 8-CPT-2OMe-cAMP and TS2/16 100 μM and 1 μg/mL, respectively. Adhesion was allowed to proceed for the indicated times at 37 °C, and unbound cells were discarded by washing three times with PBS preheated to 37 °C. Adhered cells were lysed in the wells by adding 200 μl of assay buffer containing 0.4% Triton X-100, 50 mM sodium citrate, and 10 mg/ml phosphatase substrate (Sigma-Aldrich). The total amount of cellular protein per well was quantified by acid phosphatase activity as previously described [58]. The reaction was incubated for 20 h at 37 °C and terminated by addition of 100 μl of 1 N NaOH. Absorbance was measured at 405 nm. Every condition was measured in quadruplicate.

5.9. Statistical analysis

Statistical analysis was performed in Kaleidagraph (Synergy Software) using the unpaired Student's *t*-test for samples of unequal variance.

Acknowledgements

We thank members of our labs for comments and discussion, Livio Kleij for assistance with live cell imaging experiments, Dr Jeroen Bakkers for providing the GFP-CAAX construct and Dr Mark Ginsberg for pEGFP-paxillin. We thank Dr Jan Willem Akkerman for sparing precious LIBS6 antibody, which originated from Dr Mark Ginsberg, whom we thank for it as well. We thank Arnoud Sonnenberg for support, suggestions and critical reading of the manuscript. This work was supported by a Long-Term Fellowship from the Human Frontier Science Program (KSL), and grants from the Dutch Cancer Society (KWF Kankerbestrijding) to JHR (2003–2956) and JdR (2006-3714).

Appendix A. Supplementary data

Supplementary data associated with this article can be found, in the online version, at doi:10.1016/j.cellsig.2008.01.018.

References

[1] J.P. Thiery, Nat. Rev., Cancer 2 (6) (2002) 442.
[2] E.H. Danen, Curr. Pharm. Des. 11 (7) (2005) 881.
[3] R. Horwitz, D. Webb, Curr. Biol. 13 (19) (2003) R756.
[4] M.P. Sheetz, D.P. Felsenfeld, C.G. Galbraith, Trends Cell Biol. 8 (2) (1998) 51.
[5] E. Zamir, B. Geiger, J. Cell Sci. 114 (Pt 20) (2001) 3583.
[6] D.J. Webb, J.T. Parsons, A.F. Horwitz, Nat. Cell Biol. 4 (4) (2002) E97.
[7] A.J. Ridley, M.A. Schwartz, K. Burridge, R.A. Firtel, M.H. Ginsberg, G. Borisy, J.T. Parsons, A.R. Horwitz, Science 302 (5651) (2003) 1704.
[8] A. Huttenlocher, M.H. Ginsberg, A.F. Horwitz, J. Cell Biol. 134 (6) (1996) 1551.
[9] J.P. Thiery, J.P. Sleeman, Nat. Rev., Mol. Cell Biol. 7 (2) (2006) 131.
[10] M. Deckers, M. van Dinther, J. Buijs, I. Que, C. Lowik, G. van der Pluijm, P. ten Dijke, Cancer Res. 66 (4) (2006) 2202.
[11] M. Stoker, E. Gherardi, M. Perryman, J. Gray, Nature 327 (6119) (1987) 239.
[12] J. de Rooij, A. Kerstens, G. Danuser, M.A. Schwartz, C.M. Waterman-Storer, J. Cell Biol. 171 (1) (2005) 153.
[13] A.K. Howe, Biochim. Biophys. Acta 1692 (2-3) (2004) 159.
[14] M.L. Edin, A.K. Howe, R.L. Juliano, Exp. Cell Res. 270 (2) (2001) 214.
[15] S. Kim, M. Harris, J.A. Varner, J. Biol. Chem. 275 (43) (2000) 33920.
[16] O. Dormond, C. Ruegg, Thromb. Haemost. 90 (4) (2003) 577.
[17] J. de Rooij, F.J. Zwartkruis, M.H. Verheijen, R.H. Cool, S.M. Nijman, A. Wittinghofer, J.L. Bos, Nature 396 (6710) (1998) 474.
[18] J.L. Bos, Curr. Opin. Cell Biol. 17 (2) (2005) 123.
[19] E. Caron, J. Cell Sci. 116 (Pt 3) (2003) 435.
[20] M.R. Kooistra, N. Dube, J.L. Bos, J. Cell Sci. 120 (Pt 1) (2007) 17.
[21] K. Katagiri, M. Hattori, N. Minato, S. Irie, K. Takatsu, T. Kinashi, Mol. Cell. Biol. 20 (6) (2000) 1956.
[22] E. Caron, A.J. Self, A. Hall, Curr. Biol. 10 (16) (2000) 974.
[23] K.A. Reedquist, E. Ross, E.A. Koop, R.M. Wolthuis, F.J. Zwartkruis, Y. van Kooyk, M. Salmon, C.D. Buckley, J.L. Bos, J. Cell Biol. 148 (6) (2000) 1151.
[24] K.M. de Bruyn, S. Rangarajan, K.A. Reedquist, C.G. Figdor, J.L. Bos, J. Biol. Chem. 277 (33) (2002) 29468.
[25] E.M. Lafuente, A.A. van Puijenbroek, M. Krause, C.V. Carman, G.J. Freeman, A. Berezovskaya, E. Constantine, T.A. Springer, F.B. Gertler, V.A. Boussiotis, Dev. Cell 7 (4) (2004) 585.
[26] K. Katagiri, A. Maeda, M. Shimonaka, T. Kinashi, Nat. Immunol. 4 (8) (2003) 741.
[27] K. Katagiri, M. Imamura, T. Kinashi, Nat. Immunol. 7 (9) (2006) 919.
[28] J. Han, C.J. Lim, N. Watanabe, A. Soriani, B. Ratnikov, D.A. Calderwood, W. Puzon-McLaughlin, E.M. Lafuente, V.A. Boussiotis, S.J. Shattil, M.H. Ginsberg, Curr. Biol. 16 (18) (2006) 1796.
[29] T. Hoshino, T. Sakisaka, T. Baba, T. Yamada, T. Kimura, Y. Takai, J. Biol. Chem. 280 (25) (2005) 24095.
[30] A. Glading, J. Han, R.A. Stockton, M.H. Ginsberg, J. Cell Biol. 179 (2) (2007) 247.
[31] E.S. Wittchen, J.D. van Buul, K. Burridge, R.A. Worthylake, Curr. Opin. Hematol. 12 (1) (2005) 14.
[32] M.J. Lorenowicz, M. Fernandez-Borja, P.L. Hordijk, Arterioscler. Thromb. Vasc. Biol. 27 (5) (2007) 1014.
[33] L.S. Price, A. Hajdo-Milasinovic, J. Zhao, F.J. Zwartkruis, J.G. Collard, J.L. Bos, J. Biol. Chem. 279 (34) (2004) 35127.
[34] Y. Ohba, K. Ikuta, A. Ogura, J. Matsuda, N. Mochizuki, K. Nagashima, K. Kurokawa, B.J. Mayer, K. Maki, J. Miyazaki, M. Matsuda, Embo J. 20 (13) (2001) 3333.
[35] A. Zhang, Z. Dong, T. Yang, Am. J. Physiol. Renal. Physiol. 291 (6) (2006) F1332.
[36] J.M. Enserink, A.E. Christensen, J. de Rooij, M. van Triest, F. Schwede, H.G. Genieser, S.O. Doskeland, J.L. Blank, J.L. Bos, Nat. Cell Biol. 4 (11) (2002) 901.
[37] A.E. Christensen, F. Selheim, J. de Rooij, S. Dremier, F. Schwede, K.K. Dao, A. Martinez, C. Maenhaut, J.L. Bos, H.G. Genieser, S.O. Doskeland, J. Biol. Chem. 278 (37) (2003) 35394.
[38] C. Hogan, N. Serpente, P. Cogram, C.R. Hosking, C.U. Bialucha, S.M. Feller, V.M. Braga, W. Birchmeier, Y. Fujita, Mol. Cell. Biol. 24 (15) (2004) 6690.
[39] A.L. Knox, N.H. Brown, Science 295 (5558) (2002) 1285.
[40] H. Kasai, J.T. Allen, R.M. Mason, T. Kamimura, Z. Zhang, Respir. Res. 6 (2005) 56.
[41] M.A. Esteban, M.G. Tran, S.K. Harten, P. Hill, M.C. Castellanos, A. Chandra, R. Raval, T.S. O'Brien, P.H. Maxwell, Cancer Res. 66 (7) (2006) 3567.
[42] P. Conrotto, I. Yakymovych, M. Yakymovych, S. Souchelnytskyi, J. Proteome Res. 6 (1) (2007) 287.
[43] E. van de Wiel-van Kemenade, Y. van Kooyk, A.J. de Boer, R.J. Huijbens, P. Weder, W. van de Kasteele, C.J. Melief, C.G. Figdor, J. Cell Biol. 117 (2) (1992) 461.
[44] A.L. Frelinger III, I. Cohen, E.F. Plow, M.A. Smith, J. Roberts, S.C. Lam, M.H. Ginsberg, J. Biol. Chem. 265 (11) (1990) 6346.
[45] K. Burridge, M. Chrzanowska-Wodnicka, Annu. Rev. Cell Dev. Biol. 12 (1996) 463.
[46] S. von der Hardt, J. Bakkers, A. Inbal, L. Carvalho, L. Solnica-Krezel, C.P. Heisenberg, M. Hammerschmidt, Curr. Biol. 17 (6) (2007) 475.
[47] R. Zaidel-Bar, C. Ballestrem, Z. Kam, B. Geiger, J. Cell Sci. 116 (Pt 22) (2003) 4605.
[48] D.J. Webb, C.M. Brown, A.F. Horwitz, Curr. Opin. Cell Biol. 15 (5) (2003) 614.
[49] K. Hu, L. Ji, K.T. Applegate, G. Danuser, C.M. Waterman-Storer, Science 315 (5808) (2007) 111.
[50] C.M. Brown, B. Hebert, D.L. Kolin, J. Zareno, L. Whitmore, A.R. Horwitz, P.W. Wiseman, J. Cell Sci. 119 (Pt 24) (2006) 5204.
[51] X. Cullere, S.K. Shaw, L. Andersson, J. Hirahashi, F.W. Luscinskas, T.N. Mayadas, Blood 105 (5) (2005) 1950.
[52] M.R. Kooistra, M. Corada, E. Dejana, J.L. Bos, FEBS Lett. 579 (22) (2005) 4966.
[53] W.T. Arthur, L.A. Quilliam, J.A. Cooper, J. Cell Biol. 167 (1) (2004) 111.
[54] A.M. Valles, M. Beuvin, B. Boyer, J. Biol. Chem. 279 (43) (2004) 44490.
[55] S.L. Gupton, C.M. Waterman-Storer, Cell 125 (7) (2006) 1361.
[56] T.J. Jeon, D.J. Lee, S. Merlot, G. Weeks, R.A. Firtel, J. Cell Biol. 176 (7) (2007) 1021.
[57] B. Franke, J.W. Akkerman, J.L. Bos, Embo J. 16 (2) (1997) 252.
[58] M.A. Schwartz, K. Denninghoff, J. Biol. Chem. 269 (15) (1994) 11133.